An Automatic Laser Scanning System for Accurate 3D Reconstruction of Indoor Scenes

Danrong Li, Honglong Zhang, and Zhan Song
Shenzhen Institutes of Advanced Technology
Chinese Academy of Sciences
Shenzhen, Guangdong Province, China
{dr.li; hl.zhang1; zhan.song}@siat.ac.cn

Duhu Man and Mark W. Jones
Computer Science Department
Swansea University, UK
Singleton Park, Swansea, SA2 8PP, Wales, UK
{m.duhu; m.w.jones}@swansea.ac.uk

Abstract –3D reconstruction of indoor scenes is important for lots of applications like SLAM (Simultaneous Localization and Mapping), VR (virtual reality) and AR (augmented reality) etc. This paper presents a precise and low-cost 3D reconstruction system, which consists of a laser emitter, monocular cameras and a turntable. The system is firstly calibrated to determine the intrinsic and extrinsic parameters of the camera and laser plane. By rotating the scanning device, a serial of laser strip images can be obtained. With the proposed point cloud registration algorithm, multiple 3D profiles of the target scene can be computed precisely and aligned automatically. As a result, a complete 3D model of the indoor scene with color information and high accuracy can be obtained. In the experiments, some real scenes are reconstructed and evaluated from the aspects of both visual quality and measurement accuracy.

Index Terms – Structured light system, 3D reconstruction, calibration, point cloud registration.

I. INTRODUCTION

Scene modelling is an important aspect of game design, movie making and many VR and AR applications. The basic modelling approach is to use some programming languages such as X3D, VRML, 3DS MAX and Maya etc. [1]. Artificial modeling is time-consuming and laborious, and modeling accuracy and realism cannot be guaranteed, especially for some irregular objects in real scene construction. On the contrary, 3D scanning technologies can accurately capture 3D scenes in a short time and thus are widely used for 3D modelling applications.

There are many kinds of 3D reconstruction equipment and methods, which can be divided into two types: contact type and non-contact type. The typical measuring instrument of contact type is the three coordinate measuring instrument [2], which has high precision, but is not suitable for the modeling of the scene or the precision of the object. Non-contact type reconstruction includes 3D reconstruction, photometric stereo [3, 4], stereo vision method [5, 6], SFS (Structure from Motion) [7], structured light [8, 9] and so on. These have been well developed in recent years. This system uses a low cost three-dimensional reconstruction of structured light, which compared to some of the structural light reconstruction equipment, is much more cost effective. Compared with binocular vision and the SFM algorithm, the feature points are easier to detect, and it is not necessary to measure 3D data by laser radar. Some recent RGBD cameras also have been used for the 3D reconstruction of indoor scenes [10-12], like Kinect, TOF and RealSense devices etc. But, the reconstruction accuracy is lower than approaches which are based on visual triangulation, particularly point cloud registration.

The diagram of the proposed automatic laser scanning system is shown in Fig. 1. The system consists of four components: one camera, one turntable, one laser-line projector, and mounting brackets. The laser and camera are fixed and mounted on the rotation table. During scanning, the laser-line projector remains open, the turntable starts from 0°, and the image with the laser-line is captured every α degrees. The program calculates the point cloud on the intersecting line of the laser-line plane and the surface of objects in the current camera coordinate frame according to the image captured by the camera. The turntable rotates $360/\alpha$ times to complete a complete scan. With the proposed point cloud registration algorithm, point clouds computed at various scanning positions can be automatically integrated by the transformation matrix that is calculated from system calibration. With a full rotation, a 3D model of the room with color texture can be obtained without user interactions.

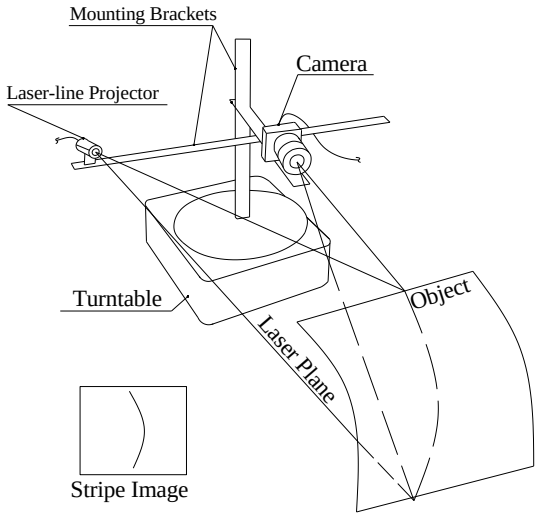

Fig. 1. Illustration of the proposed automatic 3D laser scanning system.

This work was supported in part by the National Natural Science Foundation of China (Nos. 61375041, U1613213), Shenzhen Science Plan (JCYJ20150401150223645, JSGG20150925164740726) and The CAS Key Laboratory of Human-Machine Intelligence-Synergy Systems. Duhu Man is supported by a Sêr Cymru COFUND fellowship.

II. Modeling and Calibration of the 3D System

The reconstruction model presented in this paper is based on the perspective projection and pinhole models. The relative coordinate frames are defined as follows. A point in the world coordinate frame can be transformed from the world coordinate frame to the camera frame, and then to the image frame. Ideally, there is no distortion in the lens, and the pinhole camera model is shown in Fig. 2. There are four coordinate systems defined in the 3D scanning system, i.e., O_n-X_nY_n: the 2D normalized image frame, O_u-X_uY_u: the 2D image coordinate frame, O_c-$X_cY_cZ_c$: the 3D camera coordinates frame, and O_w-$X_wY_wZ_w$: the 3D world coordinate frame. O_c is the projection center of the camera and the Z_c-axis is the optical axis of the camera lens.

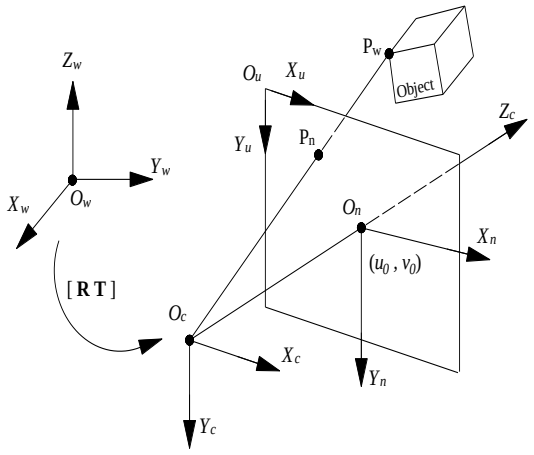

Fig. 2. Geometrical model of the 3D laser scanning system [13].

The transformation from the camera coordinate frame to the image frame can be expressed as:

$$Z_c\begin{bmatrix}u\\v\\1\end{bmatrix}=\begin{bmatrix}1/s_x & 0 & u_0\\0 & 1/s_y & v_0\\0 & 0 & 1\end{bmatrix}\begin{bmatrix}f & \gamma & 0 & 0\\0 & f & 0 & 0\\0 & 0 & 1 & 0\end{bmatrix}\begin{bmatrix}X_c\\Y_c\\Z_c\\1\end{bmatrix}$$
$$=\begin{bmatrix}a & \gamma & u_0\\0 & b & v_0\\0 & 0 & 1\end{bmatrix}\begin{bmatrix}X_c\\Y_c\\Z_c\\1\end{bmatrix}=\mathrm{A}\begin{bmatrix}X_c\\Y_c\\Z_c\\1\end{bmatrix} \quad (1)$$

where s_x and s_y represent the horizontal and vertical pixel pitch on the sensor, and (u_0, v_0) is the principle point. The image plane is located at a distance of f behind the projection center. **A** is called the intrinsic parameters matrix, α and β are the effective focal length in pixels of the camera in the x and y directions, and describes the skewness of the two axes of the image. The transformation from an image point (u, v) to the world coordinate 3D point (X_w, Y_w, Z_w) can be simplified as:

$$\begin{bmatrix}u\\v\\1\end{bmatrix}==\mathbf{A}\begin{bmatrix}\mathbf{I} & \mathbf{0}\end{bmatrix}\begin{bmatrix}\mathbf{R} & \mathbf{t}\\\mathbf{0}^{\mathrm{T}} & \mathbf{1}\end{bmatrix}\begin{bmatrix}X_w\\Y_w\\Z_w\\1\end{bmatrix}=\mathbf{A}\begin{bmatrix}\mathbf{I} & \mathbf{0}\end{bmatrix}\mathbf{H}_{\mathbf{w}}^{\mathbf{c}}\begin{bmatrix}X_w\\Y_w\\Z_w\\1\end{bmatrix} \quad (2)$$

where $\mathbf{H}_{\mathbf{w}}^{\mathbf{c}}$ is a 4×4 transformation matrix which relates the world coordinate frame to the camera coordinate frame, also called the extrinsic parameters matrix. **t** is a 3×1 translation vector and **R** is a 3×3 orthogonal rotation matrix. **R** and **t** determine the position of the camera with respect to the world, **I** is the 3×3 identity matrix, and **0** is a 3×1 zero matrix.

When considering lens distortion of camera, there are deviations between the actual projection points (u', v') and the theoretical projection points (u, v) in the image [14]. For most lenses, the distortion model can be approximated as:

$$\begin{pmatrix}u'\\v'\end{pmatrix}=\frac{2}{1+\sqrt{1-4k(u^2+v^2)}}\begin{pmatrix}u\\v\end{pmatrix} \quad (3)$$

where k models the magnitude of the radial distortions. If the distortion is pincushion-shaped, k is positive, while for barrel-shaped it is negative.

To describe the mapping of a 3D point from the world coordinate frame to the 2D image coordinate frame, the intrinsic and extrinsic parameters should be calibrated. Photogrammetric calibration and self-calibration are the two major categories in the field of calibration. The photogrammetric method needs to use a precision calibration block [15], and the intrinsic and extrinsic parameter matrices of the camera are calculated by establishing the correspondence between the points on the calibration block and the image points. Self-calibration [16] estimates intrinsic and extrinsic parameter matrices based on the correspondence between image points and does not require a calibration object with known 3D geometry. Zhang [17] proposed a flexible and high precision approach for camera calibration, requiring only the camera to observe a planar pattern which can easily be printed and placed on a rigid planar surface shown at a few (at least two) different orientations. Thereby radial lens distortion is modeled. Using his proposed procedure, the intrinsic and extrinsic parameter matrices of calibration can be solved, and the distortion correction can be calculated analytically. It is evident from (2) that only knowing the image projection point (u, v) in the image coordinate frame cannot solve the 3D point (X_c, Y_c, Z_c) in the 3D camera coordinate frame, because any point on the laser-line projection appearing within the camera field of view is a point in the laser plane. If the laser plane equation can be solved in the camera frame of reference, the laser plane can be described as:

$$ax_c+by_c+z_c=c \quad (4)$$

where a, b and c are constants describing the laser-plane equation. Then the spatial points in the camera frame corresponding to the projection point (u, v) in the image coordinate frame can be determined by (2) and (4).

Many methods exist to calibrate laser light plane. One of the common methods is to use a calibration block, which is a precisely manufactured object from which a few feature points can be obtained. Abu-Nabah [18] uses the rectangular notch calibration block successfullyby having its top surface aligned vertically to the laser plane allowing calibration of the laser line plane equation. To calibrate the structured light plane, cross-ratio invariance is also a common method. Zhou [19] proposed a novel approach to calibrate the laser plane with free-moving one-dimensional target. The camera coordinates of a control point on the light-stripe can be calculated by the feature-line equation and its distance to the origin is calculated with its projective coordinates based on a 1D projective transformation. The laser plane was then fitted to these points. A calibration approach based on active vision for a light plane was proposed by Chen [20], where the projection of parallel lines in the light plane are captured through translational motions, and the normal vector of the light plane is calculated from vanishing points. In [21], a simple calibration method for deriving the structured light plane parameters for welding robots was proposed. The laser irradiates on the calibration plate during camera calibration, because the points on the intersection of the laser plane and the surface of the object meet the pinhole model. Moreover, according to Zhang's calibration method, it assumes the model plane is on Z=0 of the world coordinate frame, and detects the sub-pixel center of the laser line $(u_i, v_i), i = 1, 2, 3...$ on the surface of the calibration plate. Therefore, the corresponding coordinates in the camera coordinate frame can be solved as follow:

$$Z_{ci} = \frac{r_{31}t_x + r_{32}t_y + r_{33}t_z}{(u_i - u_0)r_{33}/\alpha + (v_i - v_0)r_{32}\beta + r_{33}} \tag{5}$$

$$Y_{ci} = \frac{Z_{ci}(v_i - v_0)}{\beta} \tag{6}$$

$$X_{ci} = \frac{Z_c(u_i - u_0) - \gamma Y_c}{\alpha} \tag{7}$$

The laser light plane equation (4) can be fitted by using a series of laser lines on the calibration plates with different orientations as (8).

$$\min_{a,b,d} \left\| \begin{pmatrix} X_{c1} & Y_{c1} & 1 \\ \vdots & \vdots & \vdots \\ X_{ci} & Y_{ci} & 1 \end{pmatrix} \begin{pmatrix} a \\ b \\ c \end{pmatrix} - \begin{pmatrix} Z_{c1} \\ \vdots \\ Z_{ci} \end{pmatrix} \right\| \tag{8}$$

By solving (8) via a linear least squares method, the constants *a*, *b* and *c* can be uniquely identified. Therefore, according to (2) and (4), we can calculate 3D positions of the points lying on the laser strips in the captured image.

III. Alignment of Point Clouds at Different Scan Angle

In section II, the reconstructed 3D points are only defined based on the camera reference frame. While the scanning system is rotated, multiple 3D laser lines should be aligned together under the same world coordinate frame. Therefore, it is necessary to calibrate the turntable. If the installation of turntable and camera is accurate, the rotation vector coincides with the rotation axis and the camera coordinate frame will rotate around the turntable axis as shown by Fig. 3.

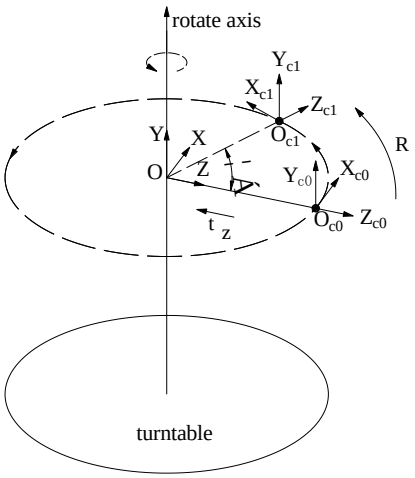

Fig. 3. The scanning system should rotate around the turntable axis.

The camera coordinate frame at a certain angle α can be converted to a fixed coordinate frame *O-XYZ* by (9).

$$\begin{bmatrix} X_c \\ Y_c \\ Z_c \\ 1 \end{bmatrix} = \begin{bmatrix} \cos\alpha & 0 & \sin\alpha & 0 \\ 0 & 1 & 0 & 0 \\ \sin\alpha & 0 & \cos\alpha & t_z \\ 0 & 0 & 0 & 1 \end{bmatrix} \begin{bmatrix} X_1 \\ Y_1 \\ Z_1 \\ 1 \end{bmatrix} \tag{9}$$

However, in practice, it is impossible to obtain the ideal mounting of bracket and camera. The camera coordinate frame doesn't revolve around the vertical support but around a rotation vector as shown by Fig. 4. It is difficult to estimate the transition matrix between O_{c0}-$X_{c0}Y_{c0}Z_{c0}$ and *O-XYZ* by manual measurement. Therefore, we propose a method to obtain the transformation matrix of the camera from different positions to the fixed coordinate system and realize the point cloud integration automatically.

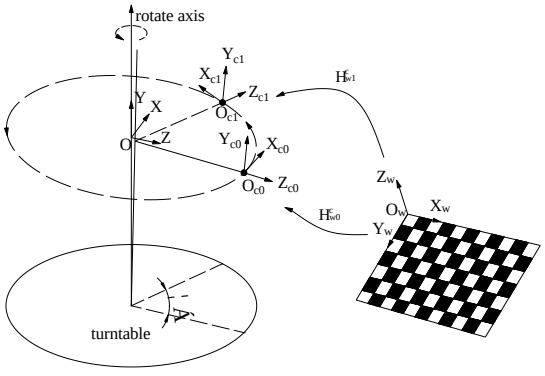

Fig. 4. The real rotation axis is not coincident with rotation table axis.

According to [17], the calibration plate plane lies on Z=0 of the world coordinate frame during calibration. The transformation matrix which relates the world coordinate frame to the camera coordinate frame was obtained after calibration. Therefore, if two cameras located at O_{c0} and O_{c1} take a fixed calibration plate respectively, we can get their transformation matrices as:

$$\begin{bmatrix} X_{c0} \\ Y_{c0} \\ Z_{c0} \\ 1 \end{bmatrix} = \mathbf{H}^{\mathbf{c}}_{\mathbf{w0}} \begin{bmatrix} X_w \\ Y_w \\ Z_w \\ 1 \end{bmatrix} \tag{10}$$

$$\begin{bmatrix} X_{c1} \\ Y_{c1} \\ Z_{c1} \\ 1 \end{bmatrix} = \mathbf{H}^{\mathbf{c}}_{\mathbf{w1}} \begin{bmatrix} X_w \\ Y_w \\ Z_w \\ 1 \end{bmatrix} \tag{11}$$

$$\begin{bmatrix} X_{c1} \\ Y_{c1} \\ Z_{c1} \\ 1 \end{bmatrix} = \mathbf{H}^{\mathbf{c}}_{\mathbf{w1}} \mathbf{H}^{\mathbf{c}\ -1}_{\mathbf{w0}} \begin{bmatrix} X_0 \\ Y_0 \\ Z_0 \\ 1 \end{bmatrix} = \mathbf{Tr} \begin{bmatrix} X_0 \\ Y_0 \\ Z_0 \\ 1 \end{bmatrix} \tag{12}$$

After obtaining the camera coordinate frame transformation matrix of a fixed rotation angle, at the angle of a=n×α (n=0, 1, 2... $\lfloor 360/a \rfloor$), the camera coordinate frame can be transformed to the fixed coordinate frame as:

$$\begin{bmatrix} X_{cn} \\ Y_{cn} \\ Z_{cn} \\ 1 \end{bmatrix} = \mathbf{Tr}^{\mathrm{n}} \begin{bmatrix} X_0 \\ Y_0 \\ Z_0 \\ 1 \end{bmatrix} \tag{13}$$

In order to improve the computation speed, $\mathbf{Tr}^{\mathrm{n}}$ is stored as a look-up-table. Therefore, the system can take pictures every α degrees. By solving each point cloud, and transferring the point cloud to a fixed camera frame, a complete 3D model can be obtained.

IV. Experimental Results

The experimental setup consists of a USB 3.0 camera with resolution of 1280×1024 pixels, and a lens with a 6mm focal length. A red line laser with an emitting angle of about 90° is used. After the scanning system is installed, the camera can be calibrated using the method of Zhang. The calibration took a total of 23 calibration plate images, of which the last four are used to fit the laser plane equation. The last two are used to estimate the rigid transformation matrix of camera before and after rotation. In order to get a more dense point cloud, this experiment takes α=0.1°. The intrinsic parameters matrix **A** and the transformation matrix **Tr** obtained by the calibration of camera are shown in Table I.

TABLE I
INTRINSIC PARAMETERS MATRIX

Parameters	α	β	u_0	v_0
Value	2894.462	2887.338	1016.814	817.261

$$\mathbf{Tr} = \begin{pmatrix} 0.9994 & 4.0e\text{-}005 & -0.0345 & -7.3403 \\ -1.845e\text{-}005 & 0.9999997 & 0.00063 & 3.1e\text{-}006 \\ 0.03458 & -0.00063 & 0.99940 & 0.21142 \\ 0 & 0 & 0 & 1 \end{pmatrix}$$

The calibration matrix of each calibration plate is obtained. The center points of laser line are extracted from the last four graphs respectively as shown in Fig. 5. According to the equations (5) - (7), we can get the 3D points (X_{ci}, Y_{ci}, Z_{ci}), i=1, 2...n in the camera coordinate system. Then, according to these points, equation (8) is used to fit the laser plane to obtain the coefficients of the laser plane equation. The laser plane coefficients are shown in Table II.

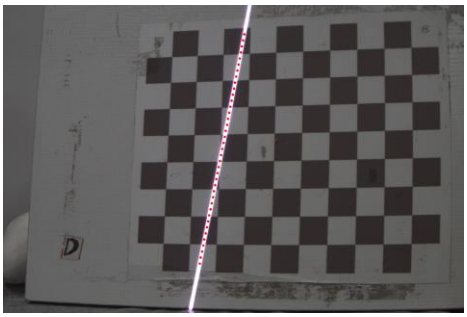

Fig. 5. Laser stripe extraction

TABLE II
LASER PLANE COEFFICIENT

Laser plane coefficient	Value
a	-7.606
b	-1.685
c	1296.203

With the laser plane equation, simultaneously the camera model can be adopted to solve the 3D coordinates of the laser line. The point of the inverse solution is compared with that of the calibration solution, and the correctness of the laser plane can be verified by the standard deviation of the two sets of data in three directions. Comparison of the two experimental results is as shown in Fig. 6, where the standard deviation of the X direction was 0.02 mm, the Y direction was 0.11 mm, and the Z direction was 1.13 mm.

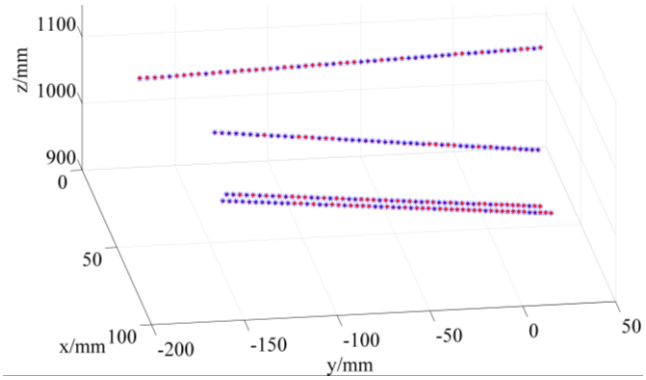

Fig. 6. Verification of plane equations and calibration. The red points are solved by external parameter matrix and blue points are solved by the camera model and laser plane equation.

To verify the system measurement accuracy, a flat glass surface is used. The glass has a distance of ~2.5 m to the camera. We selected points on the wall as a reference, with the vertical and horizontal distance between them being 300 mm. By measuring the distance between horizontal and vertical markers on the glass surface, the results show that, the average distance measured was 299.84 mm, and standard deviation was 0.87 mm.

(a)

(b)

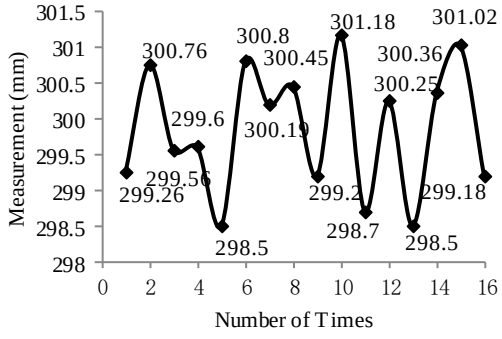

(c)

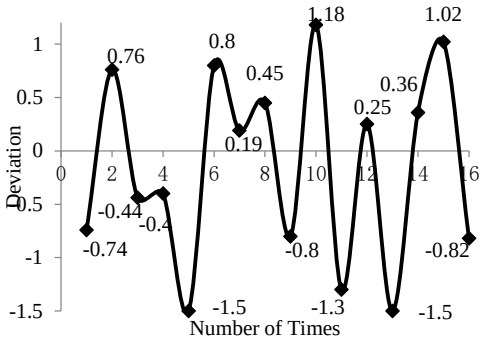

(d)

Fig. 7. Accuracy evaluation of the proposed system. (a) Flat glass wall; (b) Manual measurements between two points (300 mm); (c) Distance between points in point cloud; (d) Deviation chart.

To make the point cloud with color information, a relay and a single chip microcomputer is developed to synchronize the camera, turntable, and laser. The system can take an image with laser projection and the another image without laser projection in the same positions. Image subtraction obtains the laser stripe pattern. Next, the laser stripe extraction algorithm can be adopted to extract the stripe center. This approach improves the robustness of laser strip extraction algorithm, and also provides color information for the laser strip points. An experiment is shown in Fig. 8. Fig. 8a shows two objects with color texture, 8b shows the reconstructed 3D point clouds, and 8c shows the color 3D point clouds.

(a)

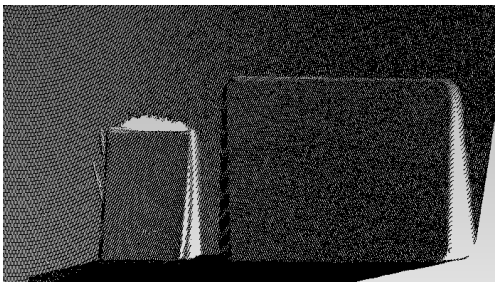

(b)

(c)

Fig. 8. Reconstruction of the scene (a) with (c) and without color (b).

By placing the scanning system in the center of a room, a full scanning is operated and the dense 3D point cloud is obtained as shown by Fig. 9. The size of the room is 3820 mm × 6150 mm. From the reconstruction results, the measured size of the room is about 3818 mm × 6141 mm. The top view of the reconstructed room scene is as shown by Fig. 9a. Two side views with and without color are displayed by Fig. 9b. A part of the room scene is enlarged and displayed in Fig. 9c.

(a)

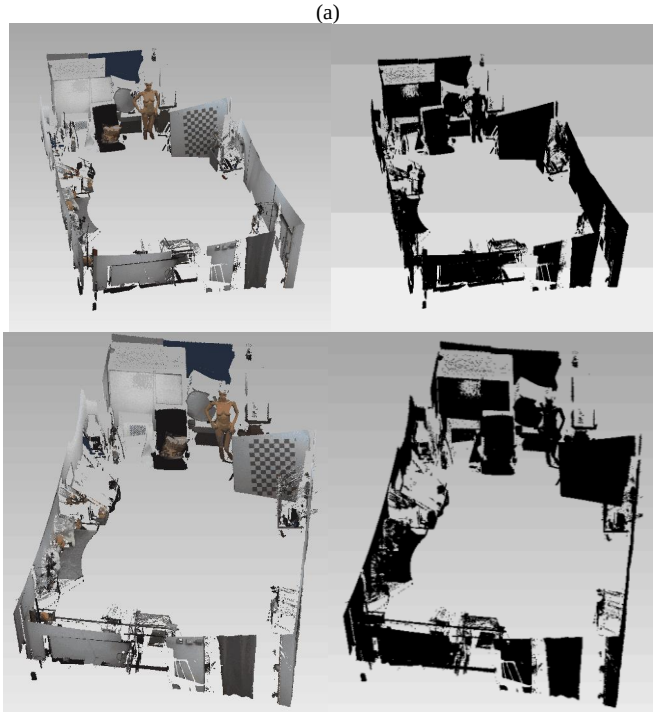

(b)

(c)

Fig. 9. 3D Reconstruction of indoor scenes. (a) Top view of reconstructed room model; (b) Side views of the reconstructed room model with and without color; (c) A close observation of part of the reconstructed room scene.

IV. Conclusion and Future Work

This paper presents an automatic and accurate 3D scanning system for the reconstruction of indoor scenes. The system works based on the laser line scanning principle. By the proposed calibration method, both camera and laser plane can be precisely calibrated. To align multiple laser profiles, a novel registration method is introduced. By the proposed laser strip detection method, both a point coordinate and its color information can be obtained. In the experiments, the measurement error can be controlled within 1 mm at a working distance of 2.5 m. With a full scanning procedure, the room scene can be reconstructed automatically with high precision. Such a system can be widely used for the indoor scene reconstruction for different applications like SLAM, VR/AR etc. Future work can address how to expand the scanning range by the usage of fisheye cameras, which will broaden the scanning range and get a more complete 3D room model.

References

[1] W. Shen and W. Zeng, "Research of VR modelling technology based on VRML and 3DSMAX," *Proceedings of 2011 International Conference on Computer Science and Network Technology*, vol. 1, pp. 487-490, Dec. 2011.

[2] Sprenger, Bernhard, "Dynamical monitoring and modelling of a coordinate measuring machine." U.S. Patent No. 9,593,927. 14 Mar. 2017.

[3] Y. Nie and Z. Song, "A novel photometric stereo method with nonisotropic point light sources," *2016 23rd International Conference on Pattern Recognition (ICPR)*, pp. 1737-1742, Dec. 2016.

[4] J. Liao, B. Buchholz, J. M. Thiery, P. Bauszat and E. Eisemann, "Indoor Scene Reconstruction Using Near-Light Photometric Stereo," in *IEEE Transactions on Image Processing*, vol. 26, no. 3, pp. 1089-1101, March 2017.

[5] N. Q. Ann, M. S. H. Achmad, L. Bayuaji, M. R. Daud and D. Pebrianti, "Study on 3D scene reconstruction in robot navigation using stereo vision," *2016 IEEE International Conference on Automatic Control and Intelligent Systems (I2CACIS)*, pp. 72-77, Oct. 2016.

[6] M. Yokozuka, K. Tomita, O. Matsumoto and A. Banno, "Accurate depth-map refinement by per-pixel plane fitting for stereo vision," *2016 23rd International Conference on Pattern Recognition (ICPR)*, pp. 2807-2812, Dec, 2016.

[7] J. Gallego and M. Pardàs, "Robust 3D SFS reconstruction based on reliability maps," *2014 IEEE International Conference on Image Processing (ICIP)*, pp. 3307-3311, Oct. 2014.

[8] E. Turner and A. Zakhor, "Automatic Indoor 3D Surface Reconstruction with Segmented Building and Object Elements," *2015 International Conference on 3D Vision*, pp. 362-370, Oct. 2015.

[9] Z. Song. "Use of structured light for three-dimensional reconstruction." The Chinese University of Hong Kong (People's Republic of China), 2008.

[10] J. W. Li, et al, "Indoor 3D scene reconstruction for mobile robots using Microsoft Kinect sensor," *2016 35th Chinese Control Conference (CCC)*, pp. 6324-6328, July, 2016.

[11] Runyang Zou, Xueshi Ge and Geng Wang, "Applications of RGB-D data for 3D reconstruction in the indoor environment," *2016 IEEE Chinese Guidance, Navigation and Control Conference (CGNCC)*, pp. 375-378, Aug. 2016.

[12] X. Chai, F. Wen, X. Cao and K. Yuan, "A fast 3D surface reconstruction method for spraying robot with time-of-flight camera," *2013 IEEE International Conference on Mechatronics and Automation*, pp. 57-62, Aug. 2013.

[13] F. Zhou, and G. Zhang. "Complete calibration of a structured light stripe vision sensor through planar target of unknown orientations." *Image & Vision Computing*, vol.23, no. 1, pp. 59-67, 2005.

[14] Lenz, Reimar, and D. Fritsch. "Accuracy of videometry with CCD sensors." *Isprs Journal of Photogrammetry & Remote Sensing* vol. 45, no. 2, pp. 90-110, 1990.

[15] Ghosh, P. K, and S. P. Mudur. "Three-Dimensional Computer Vision: A Geometric Viewpoint." *Computer Journal* vol. 38, no. 1, pp. 475-475, 1995.

[16] Pollefeys, Marc, R. Koch, and L. V. Gool. "Self-Calibration and Metric Reconstruction in Spite of Varying and Unknown Internal Camera Parameters." *International Journal of Computer Vision* vol. 32, no. 1, pp. 7-25, 1999.

[17] Z. Zhang, "A flexible new technique for camera calibration," in *IEEE Transactions on Pattern Analysis and Machine Intelligence*, vol. 22, no. 11, pp. 1330-1334, Nov 2000.

[18] Abu-Nabah, Bassam A., A. O. Elsoussi, and E. R. K. A. Alami. "Simple laser vision sensor calibration for surface profiling applications." *Optics & Lasers in Engineering* vol. 84, pp. 51-61, 2016.

[19] F. Zhou. "Calibrating Structured-light Vision Sensor with One-dimensional Target." *Journal of Mechanical Engineering* vol. 46, no.18, pp.7-12, 2010.

[20] Chen, F. Tian, M. A. Zi, and W. U. Xiang. "Calibration of light plane in line structured light sensor based on active vision." *Guangxue Jingmi Gongcheng/optics & Precision Engineering* vol.20, no. 2, pp.256-263, 2012.

[21] J. Fan, F. Jing, Z. Fang and Z. Liang, "A simple calibration method of structured light plane parameters for welding robots," *2016 35th Chinese Control Conference (CCC)*, pp. 6127-6132, July 2016.